Direct Adhesion of Endothelial Cells to Bioinspired Poly(dopamine) Coating Through Endogenous Fibronectin and Integrin $\alpha_5\beta_1$[a]

Jin-Lei Wang, Ke-Feng Ren,* Hao Chang, Fan Jia, Bo-Chao Li, Ying Ji, Jian Ji*

Mussel-inspired poly(dopamine) (PDA) coating is proven to be a simple, versatile, and effective strategy to promote cell adhesion onto various substrates. In this study, the initial adhesive behavior of human umbilical vein endothelial cells (HUVECs) is evaluated on a PDA coating under serum-free conditions. It is found that HUVECs can attach directly to and spread with well-organized cytoskeleton and fibrillar adhesions on the PDA surface, whereas cells adhere poorly to and barely spread on the control polycaprolactone surface. Endogenous fibronectin and $\alpha_5\beta_1$ integrin are found to be involved in the cell adhesion process. These findings will lead to a better understanding of interactions between cells and PDA coating, paving the way for the further development of PDA.

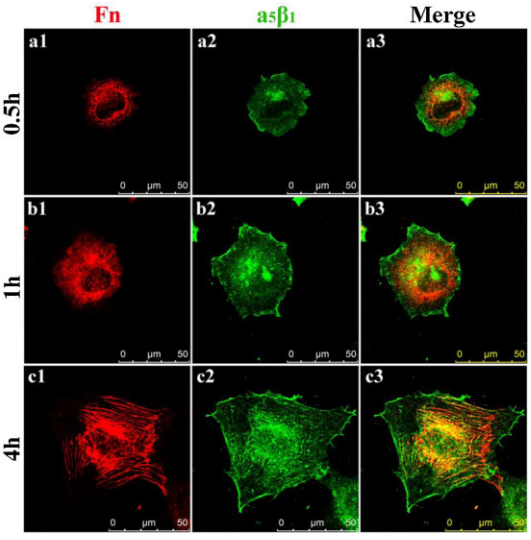

1. Introduction

The surface properties of biomaterials play important roles in the regulation of cellular behavior such as adhesion, proliferation, and differentiation.[1,2] For instance, Groth and coworkers found that preferable attachment and spreading of fibroblasts were shown on $-NH_2$ and $-COOH$ ces compared with those terminated with $-CH_3$, PEG, and $-OH$ groups.[3] Hence, tailoring the surface properties of biomaterials to achieve a specific biological response becomes one of the central questions in biomedical materials and tissue engineering.

Cell adhesion is the first cellular event that occurs when a cell comes into contact with a material surface, and it has a strong influence on the subsequent cellular events such as proliferation and differentiation.[4] Poor cell adhesion to orthopedic, dental, and cardiovascular implants may result in implant failure.[5,6] Thus, numerous surface modification strategies have been developed to improve the cell adhesion on artificial materials, such as physical adsorption, chemical immobilization of bioactive molecules, and plasma treatment.[7–9] However, these available methods have been only used to a limited extent in practical applications due to the lack of stability, requirement of multiple complicated steps, or expensive equipment.[10–12]

Recently, inspired by the bioadhesion principle of mussels, the spontaneous oxidative polymerization of dopamine in an alkaline solution has been explored as a

J.-L. Wang, Prof. K.-F. Ren, H. Chang, F. Jia, B.-C. Li, Y. Ji, Prof. J. Ji
MOE Key Laboratory of Macromolecular Synthesis and Functionalization, Department of Polymer Science and Engineering, Zhejiang University, Hangzhou 310027, China
E-mail: renkf@zju.edu.cn; jijian@zju.edu.cn

[a] **Supporting Information** is available from the Wiley Online Library or from the author.

DOI: 10.1002/mabi.201200390

simple and effective approach for the surface modification of various substrates.[13] Poly(dopamine) (PDA) has attracted great attention because it can be easily coated on any substrate irrespective of material type and shape under solvent-free and non-toxic conditions.[14] Several latest studies have shown that PDA coating could increase the affinity of various cell lines for different types of substrates.[14–17] For example, one-dimensional (1-D) electrospun polycaprolactone (PCL) nanofibers,[15] 2-D synthetic biodegradable polymer films (such as PCL, poly(L-lactide), poly(lactic-*co*-glycolic acid), poly(L-lactide-*co*-ε-caprolactone), and polyurethane),[16,17] and 3-D porous polyurethane scaffolds[16] have been modified with PDA to introduce a more cytocompatible surface. In general, PDA can promote cell adhesion mainly in two ways. In one way, PDA coating exhibits latent reactivity to various nucleophiles with amine or thiol groups,[18] so bioactive molecules (such as ECM-derived adhesion peptides and growth factors) can be efficiently immobilized on the PDA surface to enhance cell attachment and proliferation.[19,20] In the other way, PDA coating could adsorb adhesive serum proteins such as fibronectin and vitronectin from serum-containing medium. The adsorbed serum proteins maintaining their native configuration and activity could be served as recognition sites for cells adhesion and spreading.[15,16]

However, whether the PDA coating itself can directly promote cell adhesion remains unclear. Unraveling interaction between the PDA coating and cells without interference of serum proteins could pave the way for a clearer understanding and further development of PDA coating.[21] In this study, the initial adhesion of human umbilical vein endothelial cells (HUVECs) to PDA coating was investigated in serum-free medium (SFM) to avoid any disturbance of serum protein. The physical and chemical properties of the coatings were firstly characterized. We then evaluated the adhesion and spreading of HUVECs at different time points. The organization of actin cytoskeleton and formation of cell–matrix adhesions in HUVECs during the adhesion process were investigated in detail. The expression of integrins and secretion of endogenous fibronectin were also identified. Finally, the maintenance of HUVECs phenotype was examined. Interestingly, it was found that PDA coating could directly influence HUVECs adhesion through autocrine fibronectin and its $\alpha_5\beta_1$ integrins receptor, suggesting that PDA coating could serve as a cytophilic surface for cell adhesion without any help of additional ECM proteins.

2. Experimental Section

2.1. Materials

Dopamine hydrochloride was purchased from Sigma–Aldrich and used as received. PCL pellets ($\overline{M}_w = 1 \times 10^5$ g·mol^{-1}) were purchased from Jinan Daigang Biomaterial (Jinan, China). (3-Aminopropyl)triethoxysilane (APTES) (98%) was purchased from Aladdin Reagent (Shanghai, China). Rat tail collagen (Col) type I was obtained from Shengyou Biotechnology (Hangzhou, China). Human fibronectin (Fn) was purchased from Calbiochem (Merck, Darmstadt, Germany). Recombinant human vitronectin (Vn) was purchased from PeproTech (Rocky Hill, NJ, USA). Cell culture reagents were from Gibco (Invitrogen, USA). All of the chemicals and solvents used were of analytical grade.

2.2. Substrates Preparation

Glass slides with a diameter of 14 mm and one-side polished silicon wafers were cleaned with piranha solution freshly prepared from 98% H_2SO_4 and 30% H_2O_2 (3:1 v/v) for half an hour (caution: Piranha solution can react violently with many organic materials and should be handled extremely carefully!).[22]

The samples were thoroughly rinsed with MillQ water and dried under nitrogen flow. Glass slides and silicon wafers were then silanized with APTES to enhance the adhesion between PCL and the substrates.[23] In brief, after complete drying, the substrates were functionalized by immersion in 0.5% APTES in dry toluene for 30 min at room temperature. Then the slides were sequentially washed in toluene, acetone, and alcohol, dried under nitrogen flow, and finally annealed at 60 °C for 10 h.

2.3. PCL and PDA Coating

PCL was dissolved in chloroform (1% w/v solution) and spin coated (2500 rpm, 60 s, room temperature) as a thin film onto APTES treated substrates. After the spin coating process, the coated specimens were kept in fume cupboard in a clean room while allowing the solvent to evaporate. Then the PCL films were dried in a vacuum oven at 40 °C for 24 h to remove any residual solvent.

For PDA coating, the PCL films were vertically immersed in a freshly prepared dopamine solution (2 mg·mL^{-1} in 10 mM Tris-HCl, pH 8.5) for 24 h. The PDA-coated PCL films were finally rinsed extensively with ultrapure water to remove the unattached dopamine and dried under nitrogen flow.

2.4. Surface Characterization

The thickness of coatings was measured by a spectroscopic ellipsometer (M-2000, JA Woollam Co., Inc., USA) on monocrystalline silicon wafers. The static contact angles of water were measured with a DSA 100 contact angle measuring system (Krüss, Germany) using the sessile drop method (drop volume = 2 μL). Each value reported was an average of at least five independent measurements. Surface elemental compositions were analyzed by X-ray photoelectron spectroscopy (XPS) (PHI 5000C ESCA System) with Mg K_α excitation radiation ($h\upsilon = 1\ 253.6$ eV). The surface morphologies of coatings were observed by a field-emitting scanning electron microscope (FESEM) (Hitachi S-4800, Japan) and an atomic force microscope (AFM) (SPI3800N, Seiko Instrumental, Japan). Root mean squared (RMS) roughness values of

different surfaces were determined using analysis software (SPI 3800N, Seiko Instruments Inc.).

2.5. Isolation and Culture of HUVECs

Primary HUVECs were isolated from newborn umbilical cords, obtained from women with normal pregnancies according to the rules of the local ethical committee, and signed informed consent was obtained from each mother. Briefly, cells were obtained from umbilical cord treated with 1 mg · mL^{-1} collagenase (37 °C, 20 min), as previously described.[24] SFM (cat. no. 11111-044, Gibco, USA) supplemented with 10% fetal bovine serum (FBS) (Gibco), 30 μg · mL^{-1} endothelial cell growth factor supplements (ECGS) (BD), 100 IU · mL^{-1} penicillin, and 100 μg · mL^{-1} streptomycin were used as culture medium, and the medium was changed every 2 d. Cells were grown to approximately 80% confluence at 37 °C in a humidified atmosphere containing 5% CO_2, and then trypsinized to passage or for experiments.

2.6. Cell Adhesion

HUVECs at a population number between 2 and 8, and at approximately 80% confluence were washed twice with PBS, then trypsinized and washed twice with SFM. Cells were resuspended in SFM without addition of serum and ECGS and seeded on PCL-coated coverslips with or without PDA modification (14 mm diameter placed in a 24-multiwell plate) at a density of 2.5×10^4 cells · cm^{-2}. Glass slides coated with type I collagen were used as positive control. All samples were sterilized via exposure to UV light for 30 min.

2.7. SEM for Cell Morphology

For the observation of fine structure of HUVECs, the specimens were washed twice with PBS and fixed with 2.5% glutaraldehyde solution for 12 h after a certain incubation time. The specimens were then postfixed with 1% OsO_4 in phosphate buffer (pH 7.0) for 1 h and stepwise dehydrated by a graded series of ethanol (50, 70, 80, 90, 95, and 100%) for 15–20 min at each step. The dehydrated specimens were immersed in 50, 75, 90, 95% tert-butanol/ethanol solutions and pure tert-butanol (5 min each) to replace the ethanol. Finally, the samples were freeze-dried, sputtered with gold, and observed by field-emission scanning electron microscopy (FESEM) (Hitachi S-4800).

2.8. Immunofluorescent Staining

Cell seeded coverslips were rinsed twice with PBS to remove non-adherent cells. For staining of F-actin, vinculin, von Willebrand factor (vWF), vascular endothelial (VE)-cadherin, and nucleus, cells were fixed in 4% paraformaldehyde in PBS for 15 min and permeabilized in TBS (0.15 M NaCl, 50 mM Tris–HCl, pH 7.4) containing 0.2% Triton X-100 (T8787, Sigma, St. Louis, MO, USA) for 5 min. After rinsing three times with TBS, the slides were blocked with 0.1% bovine serum albumin (BSA, Sigma, St. Louis, MO, USA) in TBS for 1 h and were then incubated with mouse anti-human monoclonal antibody (1:400, V9131, Sigma, St. Louis, MO, USA), rabbit anti-human vWF polyclonal antibody (factor VIII-related antigen) (1:200, F3520, Sigma, St Louis, MO, USA) or mouse anti-Human VE-cadherin monoclonal antibody (1:200, Cat. 555661, BD Pharmingen, USA) in TBS with 0.1% BSA for 2 h at 37 °C. After washing three times with TBS, they were further incubated with Alexa Fluor 488-conjugated goat anti-mouse IgG antibody (1:500, A11029, Invitrogen, USA), Alexa Fluor 568-conjugated goat anti-rabbit IgG antibody (1:500, A11011, Invitrogen, USA) or rhodamine–phalloidin (1:800, P1951, Sigma, St. Louis, MO, USA) in TBS with 0.1% BSA for 1 h at room temperature, followed by three washes in PBS. Finally, cell nuclei were counterstained with 2 μg · mL^{-1} 4,6-diamidina-2-phenylin (DAPI) (D8417, Sigma, St. Louis, MO, USA) for 30 min at room temperature.

For staining of $\alpha_5\beta_1$, $\alpha_v\beta_3$ integrin, and fibronectin (Fn), cells were fixed in 4% paraformaldehyde in PBS for 5 min; and for staining of $\alpha_2\beta_1$ integrin, cells were fixed in methanol/acetone (1:1; –20 °C) for 10 min. After fixation, cells were permeabilized in TBS containing 0.5% Triton X-100 for 10 min. Then the coverslips were immersed in TBS containing 0.1% BSA to block the non-specific interactions. Cells on the coverslips were immunostained with mouse monoclonal antibodies against the human integrins $\alpha_5\beta_1$ (1:100, MAB1969, Chemicon, USA), $\alpha_v\beta_3$ (1:100, MAB1976Z, Chemicon, USA), $\alpha_2\beta_1$ (1:200, MAB1998Z, Chemicon, USA), or rabbit anti-human Fn polyclonal antibody (1:400, F3648, Sigma, St. Louis, MO, USA) in TBS with 0.1% BSA for 2 h at 37 °C. Thereafter the cells were stained with Alexa Fluor 568-conjugated goat anti-rabbit IgG antibody (1:500, A11011, Invitrogen, USA) or Alexa Fluor 488-conjugated goat anti-mouse IgG antibody (1:500, A11029, Invitrogen, USA) in TBS with 0.1% BSA for 1 h at room temperature. All of the samples were washed three times with TBS between each step. HUVECs cultured on Fn, Vn, and Col-coated coverslips were used as positive controls.

After staining process, the coverslips were mounted onto glass slides with antifade reagent (Prolong), and images were taken via the Leica TCS SP5 confocal microscope (Leica, Wetzlar, Germany) with 63× and 100× oil immersion objectives or via a Zeiss Axiovert 200 inverted microscope (Axio-vert 200 M, Zeiss, Germany) using 10× and 20× apochromat objectives.

2.9. Quantitative Image Analysis

To quantify cell adhesion and spreading, fluorescent images were analyzed with ImageJ software (v1.46p, NIH, Bethesda) to determine average cell density, cell spreading area and form factor, which is also called circularity (4π(area/perimeter^2)). For a perfectly smooth circle, the form factor is 1; while cells with a very high perimeter and low area lead to a value close to 0.[25] The density of adherent cells was measured by counting the number of DAPI-stained nuclei from five different areas (center, left, right, top, and bottom) in each image (magnification 100×). The projected area and form factor were obtained by measuring the actin-stained cells. More than 100 cells were measured for each group of samples.

The number and length of cell–matrix adhesions were quantified from confocal images in which cells were stained by immunofluorescence for vinculin using the NeuronJ plugin of ImageJ.[26] For each condition, at least five cells and more than 600 cell–matrix adhesions were analyzed.

In order to analyze the expression of $\alpha_5\beta_1$, $\alpha_v\beta_3$, and $\alpha_2\beta_1$ integrins quantitatively, all the images of immunofluorescence staining were

captured and processed under identical experimental conditions (exposure time, contrast, brightness, etc.). The analysis of the level of fluorescence intensity was performed using ImageJ (NIH Image) and calculated as mean fluorescence intensity per cell area in each image. At least 20 cells were analyzed for each data point.

2.10. Real-Time Reverse Transcription Polymerase Chain Reaction (Real-Time RT-PCR) Analysis

Real-time quantitative RT-PCR was performed to examine the expression profiles of adhesion specific genes for fibronectin, α_5 and β_1 integrin subunits in the HUVECs. Briefly, the cells were cultured on PCL, PDA, and collagen coating in SFM for 4 h. Total RNA was extracted by using Trizol reagent (Invitrogen, USA) according to the manufacturer's instructions and quantified by using a biophotometer (Eppendorf, Germany). The primer sequences for human fibronectin, human α_5 and β_1 integrin subunits as well as the housekeeping genes (18S rRNA) are listed in Table S1 in the Supporting Information. The real-time PCR reactions were performed with the SYBR Premix Ex-Taq Kit (Takara, Japan) and iQ qPCR system (BioRad, USA). The relative gene expression values were calculated with the comparative ΔΔCT (threshold cycle) method, and normalized against the housekeeping gene 18S.

2.11. Statistical Analysis

All data are presented as mean ± standard deviation (SD). The statistical significance was assessed by analysis of variance (ANOVA) and the Student's *t* test and the probability value of $p < 0.05$ was considered significant.

3. Results and Discussion

In order to explore the effect of PDA coating on the adhesion behavior of HUVECs, we chose PCL as a negative control. PCL is the most commonly used biodegradable polymers for tissue engineering and biomedical applications because of its slow degradability, good biocompatibility, and excellent mechanical characteristics.[27] However, due to its intrinsic hydrophobicity and lack of molecular motifs for biological recognition, PCL has poor affinity for cell adhesion and proliferation.[11] Meanwhile, type-I collagen which has been widely used to enhance cell adhesion was used as a positive control.

3.1. Characterization of Polymer Coating

PCL coating was prepared by spin coating onto APTES treated coverslips to facilitate observation of cells on the films with a

Table 1. Summary of the properties of PCL coated glass slide (glass-PCL) and PCL coated glass slide further modified with PDA (glass-PCL-PDA).

	Thickness [nm]	Contact angle [°]	RMS roughness [nm]
Glass	N/A	9.8 ± 0.7	0.30 ± 0.08
Glass-PCL	66.0 ± 3.9	72.6 ± 0.4	4.62 ± 0.76
Glass-PCL-PDA	79.1 ± 3.8	53.2 ± 1.8	4.01 ± 0.37

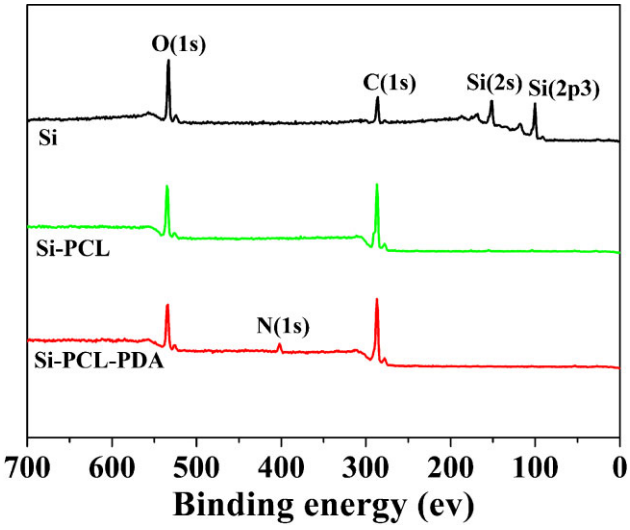

Figure 1. XPS wide scan spectra of Si substrate, Si-PCL and Si-PCL-PDA surface.

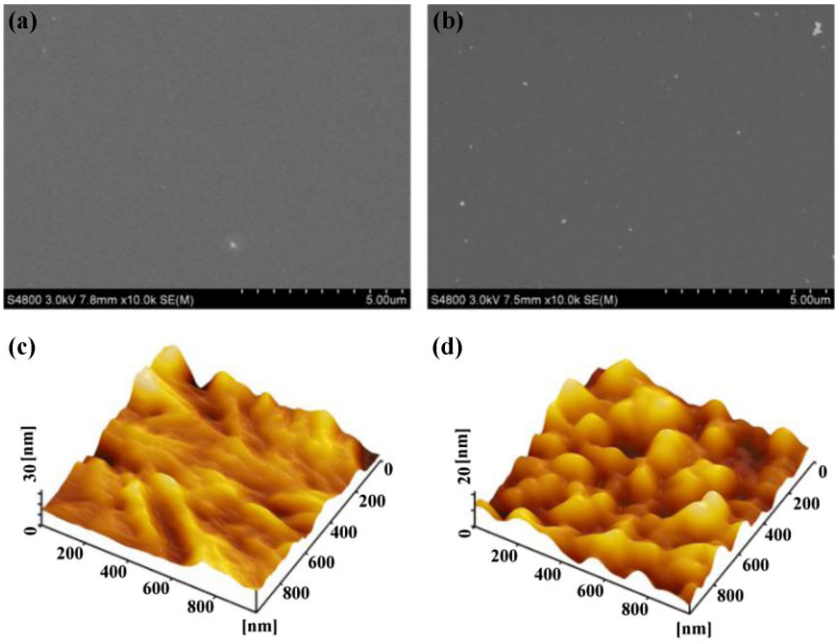

Figure 2. SEM (a, b) and AFM (c, d) images of PCL (a, c) and PCL-PDA (c, d) coatings.

laser scanning confocal microscope. A summary of the physical properties of various surfaces was given in Table 1. The changes of film thickness and static contact angles of different coatings (9.8° → 72.6° → 53.2°) indicate the presence of PCL films and the subsequent successful functionalization of PCL with PDA. There was no significant difference in the surface roughness before and after PDA modification. The thickness of PDA coating was ≈13 nm, which was in agreement with previous report.[28]

The XPS wide scan spectrum of various surfaces was showed in Figure 1. The disappearance of Si 2s and Si 2p3 signals and a significant increase in the relative intensity of C 1s signals for the PCL on the Si-wafer (Si-PCL) suggested that a uniform PCL coating was formed after spin-coating. The presence of PDA on the surface of PDA-modified PCL (Si-PCL-PDA) could be deduced from the appearance of the N 1s peak at the binding energy of about 399 eV. All these results confirmed the successful coating of PCL and the succeeding deposition of PDA on PCL surface.

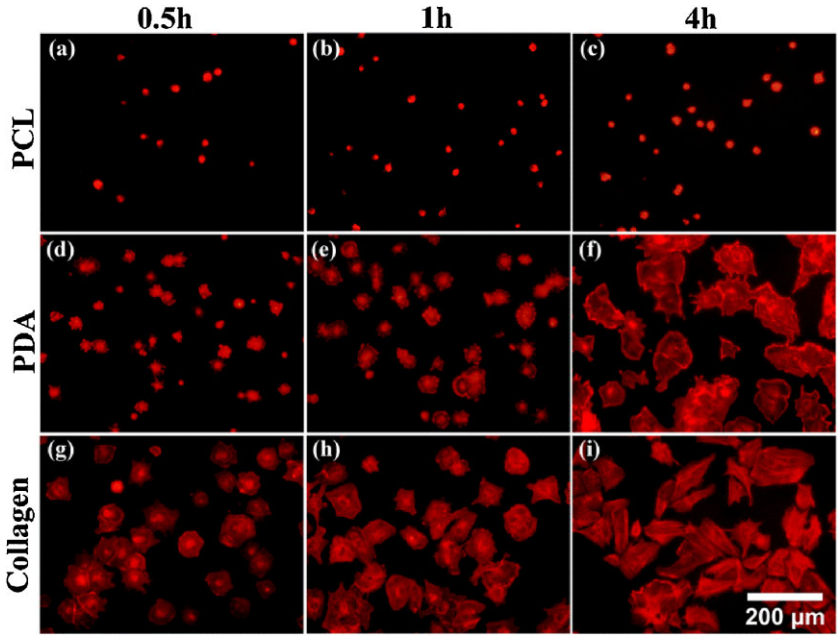

Figure 3. F-actin staining for HUVECs adhered to PCL, PDA, and collagen in SFMs for 0.5, 1, and 4 h. Scale bar = 200 μm. PDA coating itself can promote attachment and spreading of HUVECs.

The surface morphologies of PCL and PCL-PDA coatings were observed with SEM and AFM. As shown in Figure 2a,b, no significant morphological change in microscale was observed for the surfaces of PCL before and after PDA deposition from the SEM images. Nevertheless, the fine topographical feature on the nanoscale of the PCL coating shown by AFM images changed after modification of PDA. Consistent with previous research,[29] the randomly distributed nanoscale fibrous texture of PCL coating almost disappeared after PDA modification (Figure 2c and d), confirming the presence of homogeneous deposition of PDA. The PCL coating modified with PDA, for convenience, was abbreviated as PDA in the following text.

3.2. Attachment and Spreading of HUVECs

Previous reports have demonstrated that PDA could enhance the attachment and spreading of different types of cell on a variety of materials.[14–17] The main reason for the improvement of cell affinity was the adsorbed serum proteins maintaining their native configuration on the

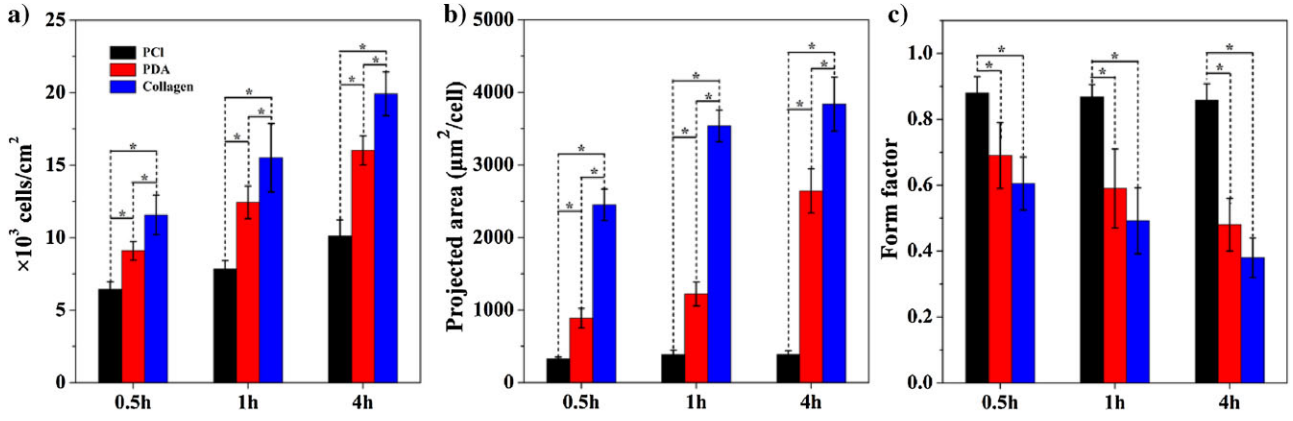

Figure 4. Quantification of cell density (a), spreading area (b), and form factor (c) of HUVECs after 0.5, 1, and 4 h of incubation on PCL, PDA, and collagen. Data are expressed as mean ± SD, * indicates significant difference at $p < 0.05$. More than 100 cells were measured for each group of samples.

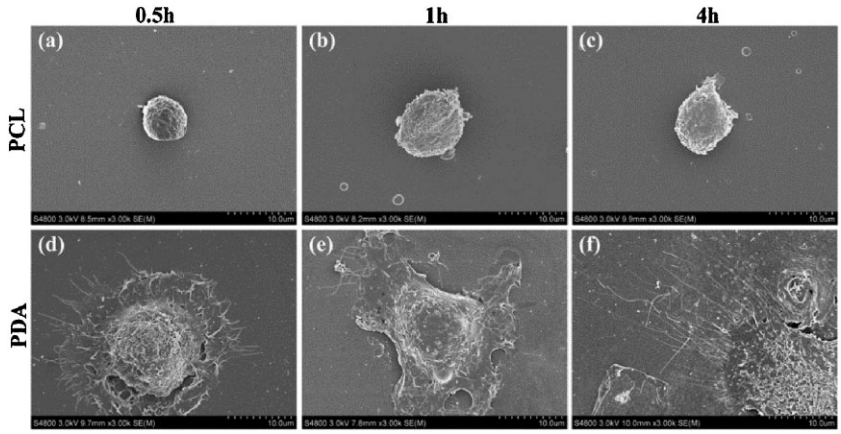

Figure 5. SEM images of HUVECs adhered to PCL and PDA for 0.5, 1, and 4 h. Obvious lamellipodia and filopodia were observed during spreading of HUVECs on the PDA surface.

PDA-coated surfaces.[14,16] However, whether the PDA coating itself can directly interact with cells to promote cell adhesion remains unclear. In the present study, initial adhesion behavior of HUVECs on PDA coating was studied systematically in SFM. We choose HUVECs because it is a most commonly used cell type in biomaterial research and has been widely used for the regeneration of vascular and bone tissues.[30,31]

We first studied the initial attachment and spreading of HUVECs on PCL, PDA, and collagen surfaces. Cells always kept a round shape and poorly spread on PCL coatings (Figure 3a–c), whereas cell projected area increased monotonically over time when spread on PDA coatings (Figure 3d–f), similar to that on collagen (Figure 3g–i). The cell density, mean spreading area and form factor were further quantified, as shown in Figure 4. Collagen surfaces

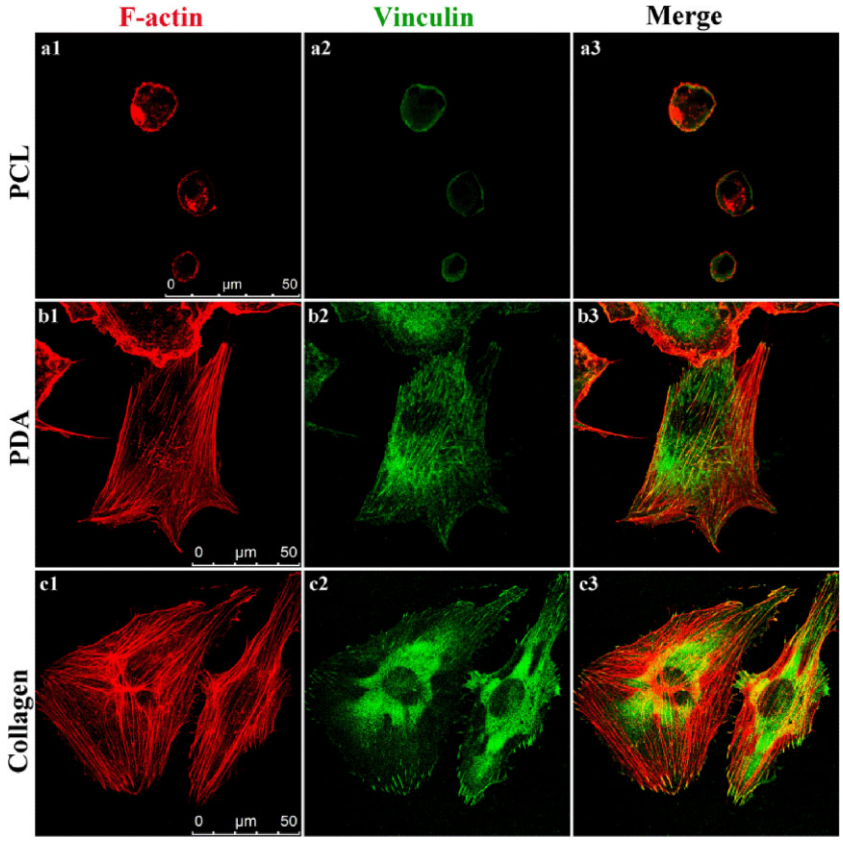

Figure 6. SEM images HUVECs adhered to PCL, PDA, and collagen for 4 h were stained for F-actin (red), vinculin (green). Scale bar = 50 μm.

always showed the highest cell density and mean spreading area. However, the cell density and cell projected area at each time point were significantly higher on the PDA coating than that on PCL (Figure 4a,b). Additionally, the form factor representing circularity of cells at each time point was significantly lower for the PDA coating than that for PCL (Figure 4c). The smaller the value of the form factor, the more elongated the cell will be. Thus, these results suggest that, without any help of additional ECM proteins, PDA cannot only directly facilitate the attachment of HUVECs, but also enable the spreading and elongation of HUVECs.

In order to better observe the initial adhesion of HUVECs to PDA coating, the ultrastructure of cell morphology at various time points was studied by SEM. The SEM images, as shown in Figure 5, were representative of typical morphologies of HUVECs adhered to PCL and PDA for 0.5, 1, and 4 h. Generally, cellular spreading is characterized by the formation of cell membrane protrusions at the leading edge, including filopodia and lamellipodia.[32] Onset of spreading of HUVECs, characterized by the generation of visible membrane protrusions, was observed after incubation for 30 min on PDA coating (Figure 5d). At the same time, cells on PCL coating displayed a small spherical shape, a typical non-spreading morphology of HUVECs (Figure 5a). Subsequently, further membrane protrusions formed, leading to rapid spreading on the PDA surface (Figure 5e,f). HUVECs on PCL, however, still remained small and rounded shape (Figure 5b,c). Consequently, PDA surface facilitated the extension of cell protrusions such as lamellipodia and filopodia, which in turn promoted cell spreading and resulted in a well-spread morphology.

3.3. Organization of Actin Cytoskeleton and Cell–Matrix Adhesions

In general, the biological processes of mammalian cell adhesion to biomaterial surfaces comprise a cascade of the following different partly overlapping events:[33] attachment, spreading, organization of the actin cytoskeleton, and formation of cell–matrix adhesions. We next investigated the actin cytoskeletal organization (actin staining) and assembly of cell–matrix adhesions (vinculin staining) of HUVECs by immunofluorescence analysis to further confirm the function of PDA coating in enhancing cell adhesion. After 4 h of adhesion, HUVECs on PDA coating exhibited well-organized actin bundles and cell–matrix adhesions similar to those shown in cells adhered to collagen (Figure 6b1–b3, c1–c3). In contrast, there was no

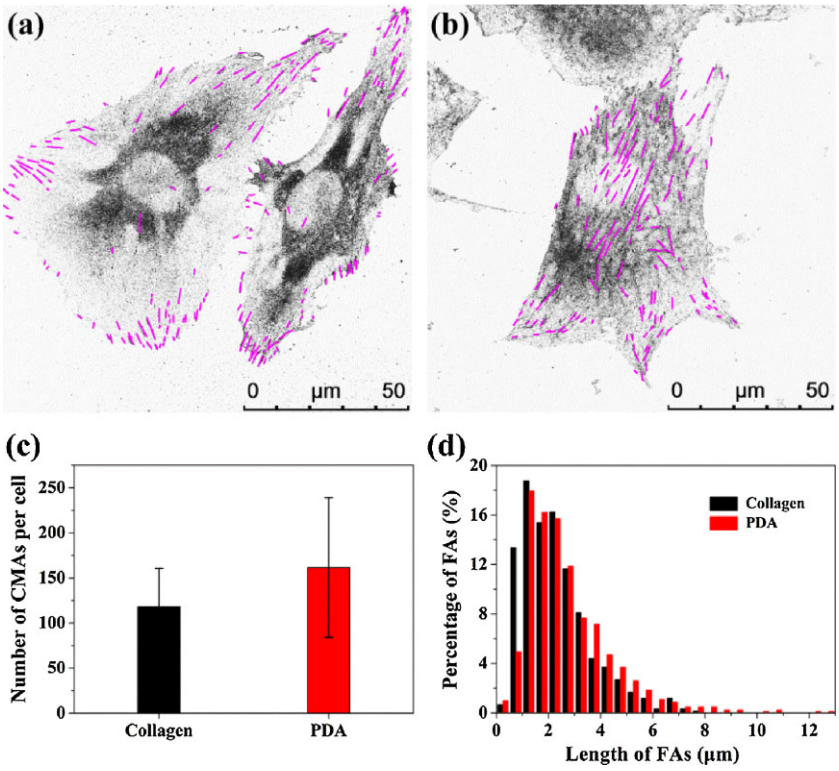

Figure 7. Spatial localization and length distribution of cell–matrix adhesions (CMAs) in HUVECs after adhesion to collagen and PDA for 4 h. Magenta spots identifies the inverted fluorescent signal of cell–matrix adhesions on the surfaces of collagen (a) and PDA (b). The scale bar represents 50 μm. Average number (c) and length distribution (d) of cell–matrix adhesions on collagen and PDA coatings. Data are expressed as mean ± SD, $n = 5$ cells and more than 600 cell–matrix adhesions were analyzed for each condition.

evidence of organization of cytoskeleton and assembly of cell–matrix adhesions for HUVECs adhered to PCL coatings (Figure 6a1–a3). F-actin could be observed in HUVECs adhered to PDA after 30 min of incubation (Supporting Information, Figure S1b1), and were clearly present after 1 h of incubation (Supporting Information, Figure S1e1). Cell–matrix adhesions were also clearly visible in HUVECs adhered to PDA after 1 h of adhesion (Supporting Information, Figure S1e2). These results indicate that, in serum-free conditions, PDA coating has similar functions as ECM proteins to facilitate organization of cytoskeleton and formation/maturation of cell–matrix adhesions.

Cell–matrix adhesions are large multi-protein assemblies which provide linkages between cells and the underlying substrate.[34] They play an important role in the process of cell attachment and spreading.[35] There are various types of cell–matrix adhesions, among which are the three major forms of cell adhesions: dot-like focal complexes (ca. 1 μm-long) located primarily at the edge of lamellipodium, elongated focal adhesions (FAs, 2–5 μm-long) often located near the periphery of cells, and fibrillar adhesions (1–10 μm-long) located predominantly in the central region of cells.[36] To understand the adhesion behavior of HUVECs on PDA better, cell–matrix adhesions at the cell–substrate interface were more clearly depicted in the inverted microphotographs (Figure 7a,b). The number and length of cell–matrix adhesions were also quantitatively analyzed. The mean length and average number of cell–matrix adhesions per cell on collagen and PDA were 2.30 ± 1.33 μm and 118 ± 43, 2.72 ± 1.68 μm and 161 ± 77, respectively. One can conclude that there was no statistically significant difference in the average number and mean length of cell–matrix adhesions. However, interestingly, it was found that the spatial localization and length distribution of cell–matrix adhesions in HUVECs adhered to collagen and PDA were different. Cells on collagen formed short FAs in the range of 1–3 μm which primarily distributed along the cell periphery (Figure 7a and d). In the case of PDA, besides short FAs, cells formed many long cell–matrix adhesions in the range of 3–7 μm located at central areas of the cell, which seemed to be fibrillar adhesions characterized by their more central location and length distribution (Figure 7b,d). It is well known that the major cell surface receptor for collagen is $\alpha_2\beta_1$ integrins, and the corresponding distribution of $\alpha_2\beta_1$

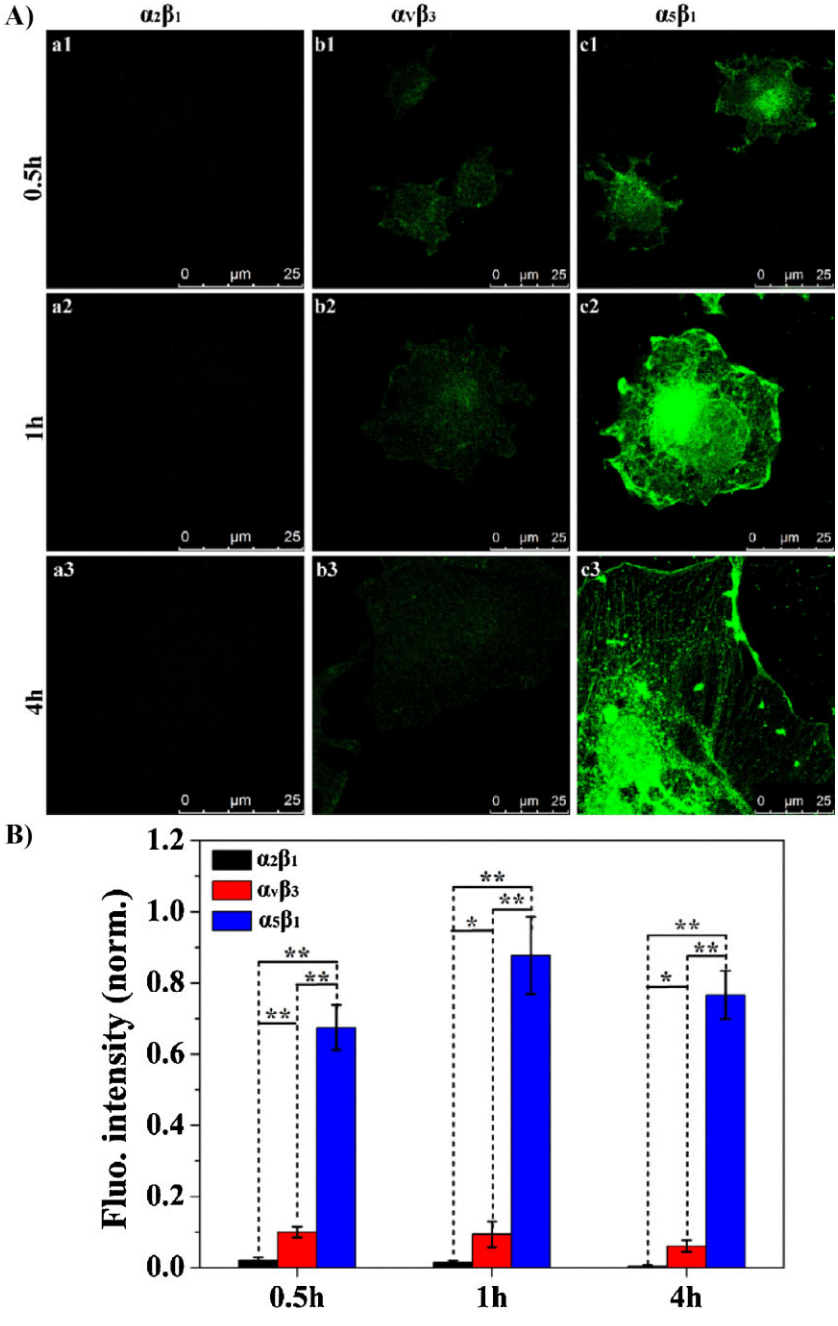

Figure 8. (A) Expression of $\alpha_2\beta_1$, $\alpha_v\beta_3$, and $\alpha_5\beta_1$ integrins in HUVECs was assessed after 4 h of adhesion onto PDA. The scale bar represents 25 μm. (B) Normalized mean fluorescence intensity of integrins at various time point. At least 20 cells were analyzed for each data point. Data are expressed as mean fluorescence intensity ± SD, * $p < 0.05$ and ** $p < 0.01$.

integrins-induced FAs is largely peripheral.[37] But the typical components of fibrillar adhesions are the fibronectin receptor $\alpha_5\beta_1$ integrin.[36] These results implied that the mechanism involved in the adhesion process of HUVECs on PDA may be different from that involved in the adhesion process of HUVECs on collagen.

3.4. Expression of Integrins

Integrins which is a superfamily of cell surface heterodimers represent the major class of cell adhesion receptors.[38] The major types of integrins involved in cell–biomaterial interactions vary with the cell types and surface properties of the biomaterials.[39] According to previous researches,[40,41] $\alpha_2\beta_1$, $\alpha_v\beta_3$, and $\alpha_5\beta_1$ integrins are the major integrins involved in the adhesion process of endothelial cells. Immunofluorescence staining of these three integrins subunits was performed to identify the main integrin that mediates cell adhesion on PDA. As shown in Figure 8A, $\alpha_5\beta_1$ integrin was strongly detected while the expression of $\alpha_v\beta_3$ integrin was very weak, and $\alpha_2\beta_1$ integrin was not detected during the initial adhesion of HUVECs on PDA. As positive controls, glass slides covered Fn, Vn, and collagen were stained for $\alpha_5\beta_1$, $\alpha_v\beta_3$, and $\alpha_2\beta_1$ integrins, respectively (Supporting Information, Figure S2). In order to quantitatively compare the results, the mean fluorescence intensity was normalized to the mean maximum intensity of the $\alpha_5\beta_1$ integrin (taken as 100%). PDA supported much higher expression level of $\alpha_5\beta_1$ integrin ($p < 0.01$) compared to the expression level of $\alpha_2\beta_1$ integrin which was negligible (Figure 8B). These results suggested that PDA facilitated the adhesion and spreading of HUVECs was mainly mediated by $\alpha_5\beta_1$ integrin. As $\alpha_5\beta_1$ integrin is one of the principal fibrillar adhesion components, the expression of $\alpha_5\beta_1$ integrin is consistent with the previous observations of fibrillar adhesion in HUVECs adhered to PDA (Figure 6b2 and 7b).

3.5. Expression of Endogenous Fn

According to the results described above, $\alpha_5\beta_1$ integrin was the main integrin expressed during the initial adhesion of HUVECs on PDA. Since the primary ligand for integrin $\alpha_5\beta_1$ is Fn which plays important roles in initial cell attachment and spreading on biomaterial surfaces.[42] We suspected that HUVECs adhered to PDA might be

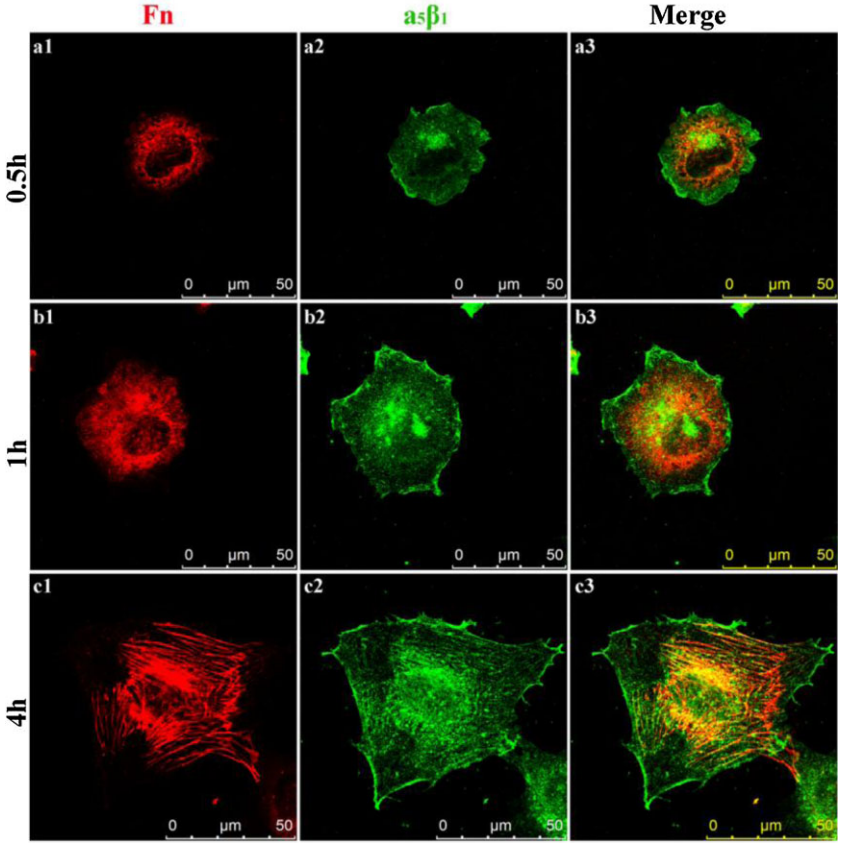

Figure 9. Expression of endogenous fibronectin and its receptor, $\alpha_5\beta_1$ integrin, during the initial adhesion of HUVECs on PDA coating. Scale bar = 50 μm.

mediated by the cooperation of autocrine Fn and $\alpha_5\beta_1$ integrin, since there was no addition of Fn in the medium. We examined the presence of endogenous Fn by immunofluorescence technique to test the hypothesis. As shown in Figure 9, endogenous Fn was secreted, accumulated, and organized into fibrillar structures during the attachment and spreading of HUVECs on PDA surfaces over time. After 4 h of cells adhesion, typical Fn fibrils were found in association with long fibrillar adhesions which were identified by their more central location and the presence of $\alpha_5\beta_1$ integrin (Figure 9c1–c3). Integrins are actively involved in the formation of the ECM as well as mediating cell adhesion, and $\alpha_5\beta_1$ is the principal integrin involved in fibronectin fibrillogenesis.[43,44] Thus the $\alpha_5\beta_1$ integrin probably contributed to the organization of autocrine Fn and adhesion of HUVECs on PDA surface. Moreover, quantitative real-time RT-PCR data analysis showed that PDA coating could significantly enhance the expression level of genes for human Fn, α_5, and β_1 integrin subunits compared with that of PCL coating (Supporting Information, Figure S3). This result further confirmed our conclusion that PDA coating facilitated the attachment and spreading of HUVECs mainly through endogenous fibronectin and integrin $\alpha_5\beta_1$. Consequently, these findings demonstrated that HUVECs synthesized and deposited Fn on the PDA surface, then the deposited Fn was assembled into fibrils in which $\alpha_5\beta_1$ integrin might act as a mediator to realize the attachment and spreading of HUVECs on the PDA coating.

3.6. Maintenance of Endothelial Phenotype

In order to study the functional development and maintenance of endothelial phenotype of HUVECs on PDA coating, we analyzed the expression of specific endothelial cell markers such as vWF and VE-cadherin.[45] As shown in Figure 10, HUVECs adhered to PDA and collagen were strongly positive for vWF and VE-cadherin compared with that of PCL. The typical endothelial marker vWF was clearly visible and well distributed within the cytoplasm and the intercellular junction protein VE-cadherin was well expressed in cell–cell adherent junctions on PDA and collagen coating. These results suggested that HUVECs adhered to PDA coating maintained a normal expression of endothelial specific proteins, indicating the maintenance

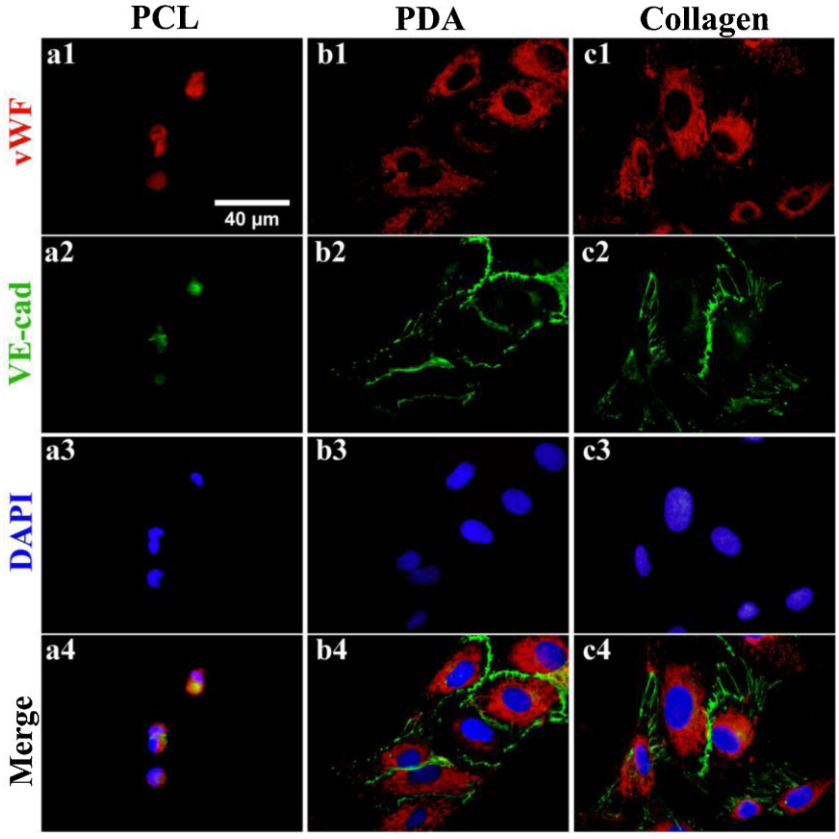

Figure 10. Immunofluorescence detection of specific endothelial markers of HUVECs adhered to PCL, PDA, and collagen for 4 h. Immunofluorescence staining of vWF (red) in the cytoplasm (a1–c1) and VE-cadherin (green) in cell–cell adherent junctions (a2–c2). The nuclei were stained with DAPI (blue, a3–c3). Scale bar = 40 μm. HUVECs adhered to PDA coating were strongly positive for vWF and VE-cadherin.

of endothelial phenotype and a good cellular compatibility of PDA coating.

4. Conclusion

In the present study, we investigated the interaction of PDA coating with HUVECs under serum free conditions. We found that PDA coating supported the attachment and spreading of HUVECs without any help of additional ECM proteins. HUVECs formed well-organized cell–matrix adhesions and fine-stretched actin bundles in 4 h of adhesion. Moreover, $\alpha_5\beta_1$ integrin was prominently expressed during the adhesion of HUVECs on PDA coating. The PDA coating facilitated the secretion, deposition and assembly of endogenous Fn, resulting in the formation of Fn fibril co-localizing with $\alpha_5\beta_1$ integrin. The interaction between Fn and $\alpha_5\beta_1$ integrin plays a key role in the adhesion of HUVECs on PDA. Moreover, PDA coating could enhance phenotypic maintenance of HUVECs compared with the control PCL. Our findings highlight that the mussel-inspired PDA can facilitate the adsorption of endogenous Fn, by which cell adhesion is triggered. It provides new insight into the functions of bioinspired PDA coating in the field of cell-based biomedical applications.

Acknowledgements: Financial support from the National Natural Science Foundation of China (50830106, 21174126, and 51103126), the China National Funds for Distinguished Young Scientists (51025312), the National Basic Research Program of China (2011CB606203), the Open Project of the State Key Laboratory of Supramolecular Structure and Materials (SKLSSM 201316), and the Research Fund for the Doctoral Program of Higher Education of China (20110101110037 and 20110101120049) are gratefully acknowledged.

Received: October 29, 2012; Revised: November 21, 2012; Published online: March 7, 2013; DOI: 10.1002/mabi.201200390

Keywords: adhesion; coatings; endothelial cells; fibronectin; poly(dopamine)

[1] S. Mitragotri, J. Lahann, *Nat. Mater.* **2009**, *8*, 15.
[2] M. Ventre, F. Causa, P. A. Netti, *J. R. Soc. Interface* **2012**, *9*, 2017.
[3] N. Faucheux, R. Schweiss, K. Lützow, C. Werner, T. Groth, *Biomaterials* **2004**, *25*, 2721.
[4] M. H. Lee, P. Ducheyne, L. Lynch, D. Boettiger, R. J. Composto, *Biomaterials* **2006**, *27*, 1907.
[5] H. Zreiqat, S. M. Valenzuela, B. B. Nissan, R. Roest, C. Knabe, R. J. Radlanski, H. Renz, P. J. Evans, *Biomaterials* **2005**, *26*, 7579.
[6] C. V. Bouten, P. Y. Dankers, A. Driessen-Mol, S. Pedron, A. M. Brizard, F. P. Baaijens, *Adv. Drug Delivery Rev.* **2011**, *63*, 221.
[7] S. R. Meyers, D. J. Kenan, X. J. Khoo, M. W. Grinstaff, *Biomacromolecules* **2011**, *12*, 533.
[8] F. J. Xu, Z. H. Wang, W. T. Yang, *Biomaterials* **2010**, *31*, 3139.
[9] A. Martins, E. D. Pinho, S. Faria, I. Pashkuleva, A. P. Marques, R. L. Reis, N. M. Neves, *Small* **2009**, *5*, 1195.
[10] A. E. Elcin, Y. M. Elcin, *Tissue Eng.* **2006**, *12*, 959.
[11] S. Yuan, G. Xiong, X. Wang, S. Zhang, C. Choong, *J. Mater. Chem.* **2012**, *22*, 13039.
[12] S. H. Hsu, C. H. Lin, C. S. Tseng, *Biofabrication* **2012**, *4*, 015002.
[13] H. Lee, S. M. Dellatore, W. M. Miller, P. B. Messersmith, *Science* **2007**, *318*, 426.
[14] S. H. Ku, J. Ryu, S. K. Hong, H. Lee, C. B. Park, *Biomaterials* **2010**, *31*, 2535.
[15] S. H. Ku, C. B. Park, *Biomaterials* **2010**, *31*, 9431.
[16] W. B. Tsai, W. T. Chen, H. W. Chien, W. H. Kuo, M. J. Wang, *Acta Biomater.* **2011**, *7*, 4187.
[17] Y. M. Shin, Y. B. Lee, H. Shin, *Colloids Surf., B Biointerfaces* **2011**, *87*, 79.
[18] H. Lee, J. Rho, P. B. Messersmith, *Adv. Mater.* **2009**, *21*, 431.
[19] C. K. Poh, Z. L. Shi, T. Y. Lim, K. G. Neoh, W. Wang, *Biomaterials* **2010**, *31*, 1578.
[20] K. Yang, J. S. Lee, J. Kim, Y. B. Lee, H. Shin, S. H. Um, J. B. Kim, K. I. Park, H. Lee, S.-W. Cho, *Biomaterials* **2012**, *33*, 6952.
[21] R. Langer, D. A. Tirrell, *Nature* **2004**, *428*, 487.
[22] N. Esman, A. Peled, R. Ben-Ishay, Y. Kapp-Barnea, I. Grigoriants, J. P. Lellouche, *J. Mater. Chem.* **2012**, *22*, 2208.
[23] O. Pop-Georgievski, S. Popelka, M. Houska, D. Chvostova, V. Proks, F. Rypacek, *Biomacromolecules* **2011**, *12*, 3232.
[24] E. A. Jaffe, R. L. Nachman, C. G. Becker, C. R. Minick, *J. Clin. Invest.* **1973**, *52*, 2745.
[25] M. T. Frey, I. Y. Tsai, T. P. Russell, S. K. Hanks, Y. I. Wang, *Biophys. J.* **2006**, *90*, 3774.
[26] E. Meijering, M. Jacob, J. C. F. Sarria, P. Steiner, H. Hirling, M. Unser, *Cytometry A* **2004**, *58*, 167.
[27] M. A. Woodruff, D. W. Hutmacher, *Prog. Polym. Sci.* **2010**, *35*, 1217.
[28] J. H. Jiang, L. P. Zhu, L. J. Zhu, B. K. Zhu, Y. Y. Xu, *Langmuir* **2011**, *27*, 14180.
[29] Y. M. Shin, Y. B. Lee, S. J. Kim, J. K. Kang, J. C. Park, W. Jang, H. Shin, *Biomacromolecules* **2012**, *13*, 2020.
[30] N. Koike, D. Fukumura, O. Gralla, P. Au, J. S. Schechner, R. K. Jain, *Nature* **2004**, *428*, 138.
[31] C. Correia, W. L. Grayson, M. Park, D. Hutton, B. Zhou, X. E. Guo, L. Niklason, R. A. Sousa, R. L. Reis, G. Vunjak-Novakovic, *PLoS One* **2011**, *6*, e28352.
[32] H. Kim, F. Nakamura, W. Lee, Y. Shifrin, P. Arora, C. A. McCulloch, *Am. J. Physiol. Cell Physiol.* **2010**, *298*, C221.
[33] U. Hersel, C. Dahmen, H. Kessler, *Biomaterials* **2003**, *24*, 4385.
[34] S. I. Fraley, Y. Feng, R. Krishnamurthy, D.-H. Kim, A. Celedon, G. D. Longmore, D. Wirtz, *Nat. Cell. Biol.* **2010**, *12*, 598.
[35] A. L. Berrier, K. M. Yamada, *J. Cell. Physiol.* **2007**, *213*, 565.
[36] B. Geiger, A. Bershadsky, R. Pankov, K. M. Yamada, *Nat. Rev. Mol. Cell. Biol.* **2001**, *2*, 793.
[37] G. Bix, J. Fu, E. M. Gonzalez, L. Macro, A. Barker, S. Campbell, M. M. Zutter, S. A. Santoro, J. K. Kim, M. Hook, C. C. Reed, R. V. Iozzo, *J. Cell. Biol.* **2004**, *166*, 97.
[38] J. D. Humphries, A. Byron, M. J. Humphries, *J. Cell. Sci.* **2006**, *119*, 3901.
[39] B. G. Keselowsky, D. M. Collard, A. J. Garcia, *Proc. Natl. Acad. Sci. USA* **2005**, *102*, 5953.
[40] J. H. Paik, S. S. Chae, M. J. Lee, S. Thangada, T. Hla, *J. Biol. Chem.* **2001**, *276*, 11830.
[41] Y. Yano, J. Geibel, B. E. Sumpio, *J. Cell. Biochem.* **1997**, *64*, 505.
[42] R. Pankov, K. M. Yamada, *J. Cell. Sci.* **2002**, *115*, 3861.
[43] E. H. Danen, P. Sonneveld, C. Brakebusch, R. Fassler, A. Sonnenberg, *J. Cell. Biol.* **2002**, *159*, 1071.
[44] J. E. Schwarzbauer, J. L. Sechler, *Curr. Opin. Cell. Biol.* **1999**, *11*, 622.
[45] M. I. Santos, S. Fuchs, M. E. Gomes, R. E. Unger, R. L. Reis, C. J. Kirkpatrick, *Biomaterials* **2007**, *28*, 240.